Journal of Alloys and Compounds 509 (2011) 5935–5941

Contents lists available at ScienceDirect

Journal of Alloys and Compounds

journal homepage: www.elsevier.com/locate/jallcom

Investigation of switching phenomenon of $Se_{75}Te_{25-x}Ga_x$ amorphous system

N.A. Hegab, I.S. Yahia, A.M. Shakra*, A.E. Bekheet, A.M. AL-Ribaty

Department of Physics, Faculty of Education, Ain Shams University, Roxy, Cairo, Egypt

ARTICLE INFO

Article history:
Received 5 August 2010
Received in revised form 2 March 2011
Accepted 3 March 2011
Available online 10 March 2011

Keywords:
Chalcogenide glasses
Se–Te–Ga
Amorphous thin film
Switching phenomenon
Electrothermal model

ABSTRACT

Thin film samples of different thicknesses ranging from 185 to 630 nm, were prepared from the synthesized amorphous $Se_{75}Te_{25-x}Ga_x$ ($0 \leq x \leq 15$ at.%) chalcogenide glass compositions by thermal evaporation technique. X-ray analysis showed that the amorphous nature of the obtained films. Investigations of the current–voltage (I–V) characteristics of amorphous films are typical for a memory type switch. The conduction activation energy (ΔE_σ) was calculated from the temperature dependence of the sample resistance of the studied films in the temperature range (293–333 K) below the glass transition temperature. The mean value of the threshold switching voltage $\bar{V}_{th}$ increases linearly with increasing film thickness and decreases exponentially with temperature (below T_g) for all investigated compositions. The threshold voltage activation energy ε_{th} was calculated from the temperature dependence of $\bar{V}_{th}$ of the studied films. The switching phenomenon observed in these films is explained in accordance with the electrothermal model for the switching process. The effect of Ga content on the studied parameters was also investigated.

© 2011 Elsevier B.V. All rights reserved.

1. Introduction

Chalcogenide glasses are an important class of amorphous materials as they behave as semiconductors and hence it can be used for producing semiconductor devices similar to crystalline ones. Studies of the physical properties of these glasses are strongly dependent on composition. In recent years great efforts are being made to produce stable glasses which have good photosensitive properties so that they are used in various solid state devices [1–3].

Amorphous materials of Se–Te based on Se have become commercial, scientifical and technological importance. It is due to their greater hardness, higher crystallization temperature, and smaller aging effects compared to pure selenium [4]. It is found that the physical properties of these materials are highly compositional dependent [5–12]. These materials are widely used in many fields as optical recording media because of their excellent laser writer sensitivity, xerography and electrographic applications, such as photoreceptors in photocopying and laser printing, infrared spectroscopy and laser fiber techniques [13–17].

It is found that the addition of some impurities to binary chalcogenide glasses changes their structure and new properties are expected for these glasses. From this point of view, the addition of Ga to Se–Te binary system can markedly affect its structural, electrical and optical properties [18–21]. It is found that Ga addition can be alloyed with most materials and has been used as a component of low melting alloys [22] because it has a low melting point (301 K) and a very high boiling point (2676 K) it has also become an attractive material as a substrate because of its good lattice matching with solid solutions of III–VI semiconductors, which are useful for the fabrication of solid state devices. Several authors have been investigated some physical properties of gallium doped chalcogenide glasses in details [18–21,23].

Okuda et al. [24] report erasable laser recording properties of a-Ga–Se–Te system and have attempted to prepare an optical disc for optical data storage. Matsushita et al. [25] have discussed a similar optical storage application for the a-Ga–Se–Te system. Rhee et al. [26] have also observed a reversible phase change (amorphous to crystalline) in thin films of this system. Also Kumar et al. [27] studied the temperature and frequency dependence of the dielectric constant and dielectric loss for bulk samples in different compositions of the Se–Te–Ga system. Measurements of dc conductivity, photoconductivity as a function of temperature and incident light intensity have been done also [28,29].

The switching phenomenon is one of the numerous interesting effects arising in strong electric field. The phenomenon, first reported by Ovshinsky [12], and observed in a great number of amorphous chalcogenide semiconductors [30–32].

Electrical switching is a rapid and reversible transition between highly resistive OFF-state and conductive ON-state driven by external electric field and characterized by a threshold voltage. There are two types of the switching state threshold switching and memory switching type. In threshold switching type the ON-state presents only under bias of some minimum holding voltage while current flows down, whereas in memory type, the ON-state is

* Corresponding author.
E-mail address: amshakra@yahoo.com (A.M. Shakra).

0925-8388/$ – see front matter © 2011 Elsevier B.V. All rights reserved.
doi:10.1016/j.jallcom.2011.03.016

permanent until a suitable reset current pulse is applied across the sample. Different mechanisms have been proposed to explain the phenomenon of electrical switching in chalcogenide glasses. These include electronic [33], thermal [34], and electrothermal [35] mechanisms.

From the above advantages of Se–Te binary system, we choose $Se_{75}Te_{25}$ as a member of Se–Te system with addition of Ga at the cost of Te. An experimental investigation have been made to study the effect of Ga addition in $Se_{75}Te_{25-x}Ga_x$ films ranged as ($0 \le x \le 15$ at.%) on the switching phenomenon and the parameters affecting the threshold voltage to identify the suitable switching mechanism.

2. Experimental details

a-$Se_{75}Te_{25-x}Ga_x$ (x = 0, 5, 10 and 15%) glasses were prepared by the melt quenching technique. Appropriate amounts of 99.999% purity elements were weighted in accordance with their atomic percentage and loaded in a silica tube (length 15 mm, internal diameter 12 mm), which was then sealed under vacuum (10^{-5} Torr). The content of each tube was heated gradually in an oscillatory furnace where the temperature was increased at the rate of 5 K/min up to 1100 K. The tubes were then kept at this temperature for 10 h with frequent rocking to ensure the homogeneity of the melt. The molten materials were quenched in ice water.

The quenched sample a-$Se_{75}Te_{25-x}Ga_x$ was taken out by breaking the silica ampoules. The amorphous nature of the glassy samples was verified by X-ray diffraction. Thin film samples were prepared from the bulk materials by thermal evaporation technique under vacuum (10^{-5} Torr) using a coating unit (Edwards E306A), onto well cleaned glass substrates for structure identification and highly polished pyrographite substrates for switching measurements. The film thickness was determined by the Tolansky interference method [36]. Samples with different thicknesses ranging from 185 to 630 nm were prepared under the same evaporation conditions.

The amorphous nature of the glassy samples was investigated by Philips X-ray unit (PW1710) using copper target with Ni filter. X-ray tube was operated at 40 kV and 55 mA. X-ray diffraction patterns measured at room temperature in the angular range from 4° to 90°.

Differential thermal analysis was used to determine the glass transition temperatures and crystallization temperatures at a heating rate of 10°/min, using Shimadzu DTA-50 equipment.

Measurements of the current–voltage (*I–V*) characteristics were carried out in a measuring cell fitted with two electrodes, the lower one was a circular brass disk in contact with the pyrographite substrate with area 2.2×10^{-2} m^2 and the upper electrode was a movable platinum wire with a thin circular end of diameter 2×10^{-4} m which provides a gentle and good contact with the upper surface of the film using a weak spring. The pressure provided by the upper electrode as well as the point of contact was kept constant through out the measurements. The measuring cell was introduced in a simple *I–V* electrical circuit. The measurements were carried out using a digital electrometer (Keithley type E616A) for the potential drop measurements and a micro digital multimeter (HC-5010-EC) for measurements of the current passing through the sample. All electrical measurements were made at room temperature as well as at different elevated temperatures using a cylindrical furnace, the temperature of which was determined using a chromel alumel thermocouple. It must be noticed that all the following measurement were carried out in the temperature range below the corresponding T_g to obtain data for amorphous state.

3. Results and discussion

3.1. X-ray characterization and differential thermal analysis

X-ray diffraction patterns for $Se_{75}Te_{25-x}Ga_x$ ($0 \le x \le 15$) films nearly of the same thickness are illustrated in Fig. 1. This figure shows the amorphous nature of the deposited films. The same behavior was obtained for other films of the studied compositions. The amorphous structure of the deposited films on substrates kept at room temperature is expected because in the deposition process, the evaporated molecules precipitate randomly on the surface of the substrate and all the following condensed molecules also adhere randomly leading to disordered films of increased thickness. The loss of adequate kinetic energy for the precipitated molecules keeps them unable to orient themselves to produce the chain structure, required for the crystalline structure. The internal stresses required of the hot molecules on the cold pre-deposited layers increase both the disorder and the degree of randomness, which yields amorphous films whatever is their thickness.

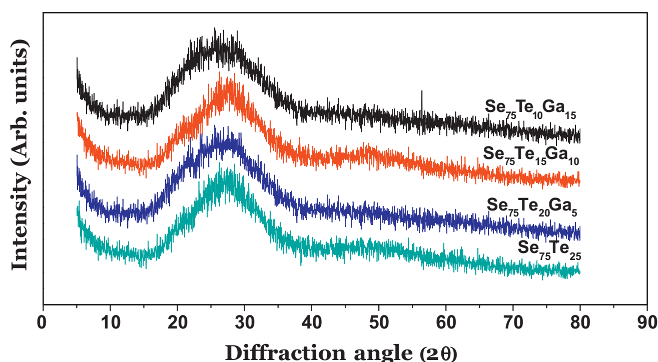

Fig. 1. X-ray diffraction patterns for all investigated film samples of nearly the same thickness.

Table 1
Values of T_g and T_c for $Se_{75}Te_{25-x}Ga_x$ ($0 \le x \le 15\%$) glasses.

Composition	T_g (K)	T_c (K)
$Se_{75}Te_{25}$	351	387
$Se_{75}Te_{20}Ga_5$	346	385
$Se_{75}Te_{15}Ga_{10}$	344	383
$Se_{75}Te_{10}Ga_{15}$	343	382

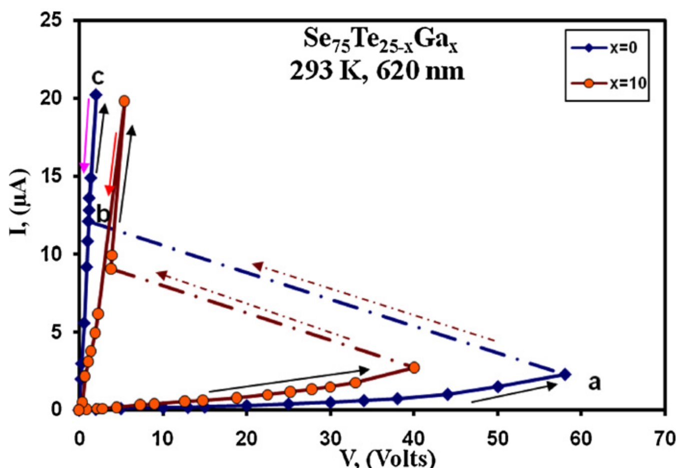

Fig. 2. Static *I–V* characteristics curves for $Se_{75}Te_{25}$ and $Se_{75}Te_{15}Ga_{10}$ films of nearly the same thickness at room temperature(293 K).

DTA analysis was carried out at a constant heating rate (10°/min). The glass transition temperature values T_g for the studied composition are estimated from the obtained thermograms and presented in Table 1. It must be noticed that all measurements in the following sections were carried out for each composition at temperature value below the corresponding T_g. It is clear from this table that the change of composition has a noticeable effect on T_g values.

3.2. I–V characteristics

The room temperature *I–V* characteristics for the investigated compositions were studied for film samples of different thicknesses (185–630 nm). Fig. 2 shows illustrative examples for the static *I–V* curve of $Se_{75}Te_{25}$ and $Se_{75}Te_{15}Ga_{10}$ films. From this figure, it is clear that the obtained curves are typical for a memory switch which is also obtained for other films of the studied compositions. It is

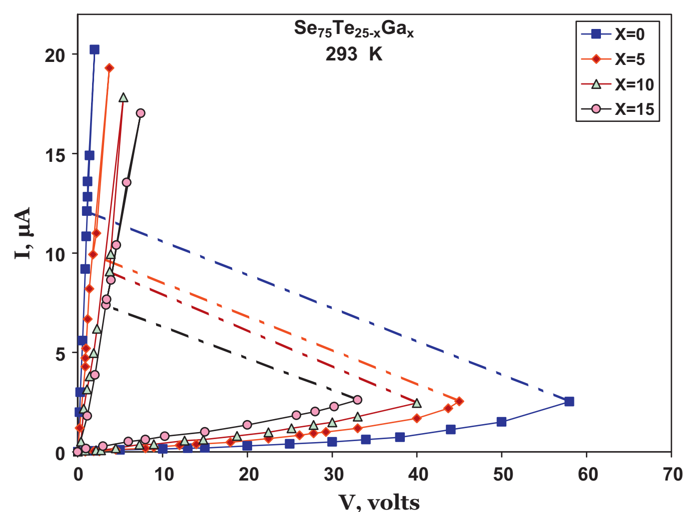

Fig. 3. Room temperature I–V characteristic curves for $Se_{75}Te_{25-x}Ga_x$ ($0 \le x \le 15$) films of approximately the same thickness (620 ± 5nm).

observed also that on increasing the applied voltage the current increases slowly forming the first branch (*oa*) of the *I–V* curve which extends to a critical voltage (corresponding to the point *a*) at which a sudden increase in the current and consequent decrease in voltage takes place, i.e. switching occurs. This critical value of the applied voltage is called the threshold voltage and the region (*oa*) on the curve is called the OFF-state of the switch. Since, the switching process takes place in a very short time (10^{-9} s) [12], it is impossible to record any reading during this time (the part *ab* of the curve). Thus, current and voltage values could be recorded only at the beginning and at the end of the switching process (points *a* and *b* on the curve). Further increase in the applied voltage increases the current passing through the sample without any significant increase in the potential drop across the sample (the part *bc*). This part is called the ON-state of the switch. When the voltage applied to the sample in the ON-state at point c is decreased the current decreases to zero following the load line along the part (*co*). If the voltage is further increased and then decreased the current increases along *oc* then decreases along *co*, i.e. the investigated films sustain their high conduction state after switching even in the absence of the applied field. Here, a structure change takes place in the microcrystalline state during the lock-on period after the device has switched to the ON-state and the current filament had been formed. The crystallization is believed to be caused by Joule heating due to high field and excess carrier concentration in the current path [37,38]. The OFF-state can be recovered by a short reset pulse, so that the crystallites redissolve into the homogeneous and stable amorphous material. Rapid cooling which follows the brief reset pulse restores the high resistance amorphous state of the material.

It must be noted that the *I–V* curves for the investigated film compositions were measured at different points uniformly distributed through out the whole surface of the film, and hence the mean value of the threshold voltage was calculated ($\bar{V}_{th}$).

Moreover, *I–V* characteristic curves for all the investigated compositions of approximately the same thickness (620 ± 5 nm) at 293 K are illustrated in Fig. 3. It is clear that the threshold voltage decreases with increase of Ga content. This is in agreement with the decrease in T_g.

The activation energy of conduction ΔE_σ has been calculated for thin film samples of the studied compositions. This is carried out by plotting the temperature dependence of the sample resistance *R* as shown in Fig. 4(a) within the linear part of the OFF-state of the *I–V* curves of the studied films, through

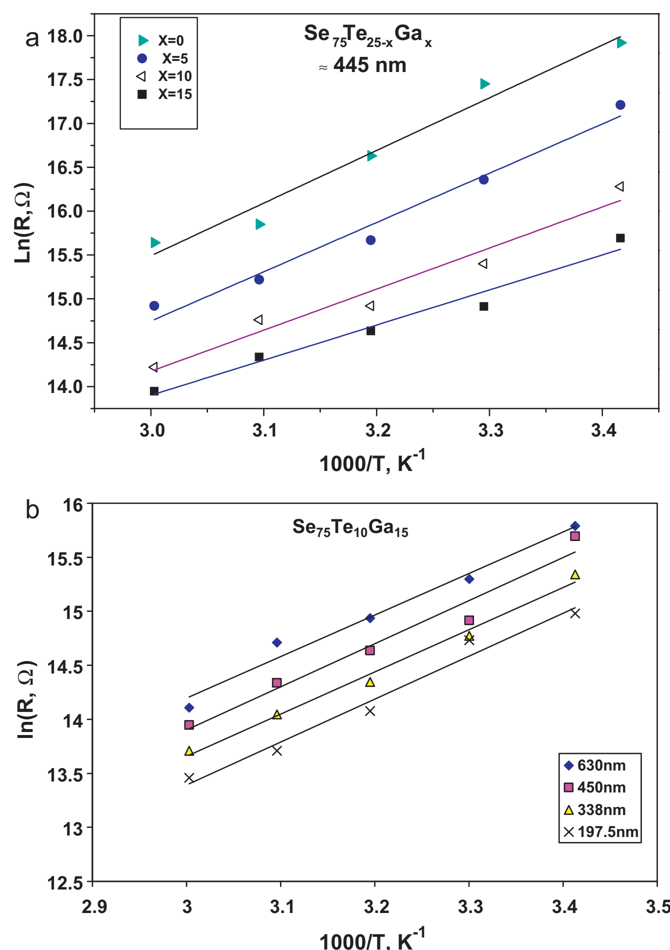

Fig. 4. (a) Temperature dependence of the resistance R for $Se_{75}Te_{25-x}Ga_x$ ($0 \le x \le 15$) films at nearly the same thickness (≈445 nm). (b) Temperature dependence of the resistance R for $Se_{75}Te_{10}Ga_{15}$ films of different thicknesses.

Table 2
Values of ΔE_σ for $Se_{75}Te_{25-x}Ga_x$ ($0 \le x \le 15\%$) films.

Composition	ΔE_σ (eV)
$Se_{75}Te_{25}$	0.51 ± 0.0133
$Se_{75}Te_{20}Ga_5$	0.49 ± 0.0038
$Se_{75}Te_{15}Ga_{10}$	0.40 ± 0.008
$Se_{75}Te_{10}Ga_{15}$	0.33 ± 0.0093

out the temperature range (293–333 K) according to the relation:

$$R = C \exp\left(\frac{\Delta E_\sigma}{k_B T}\right), \tag{1}$$

where *C* is a constant, k_B is the Boltzmann's constant and *T* is the absolute temperature. The obtained relations (ln *R* against 1000/*T*) are shown in Fig. 4(a), for nearly the same thickness of each composition as an example, yield straight lines, the slope gives the value of ΔE_σ which has single value for the studied compositions. Fig. 4(b) represent the relation $\ln R = f(1000/T)$ for different thicknesses of the $Se_{75}Te_{10}Ga_{15}$ composition as an example. It is found that ΔE_σ is independent of film thickness in the investigated thickness range. The same behavior was obtained for other compositions. Values of ΔE_σ for films under test are listed in Table 2. It is indicated from this Table that ΔE_σ decreases with Ga addition.

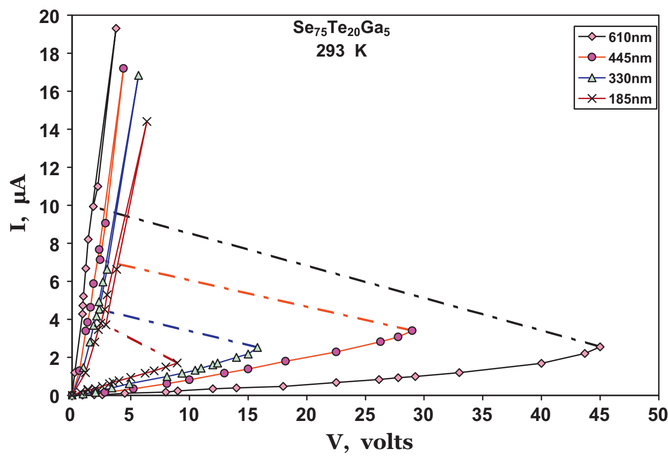

Fig. 5. Room temperature *I*–*V* characteristic curves of $Se_{75}Te_{20}Ga_5$ films of different thicknesses.

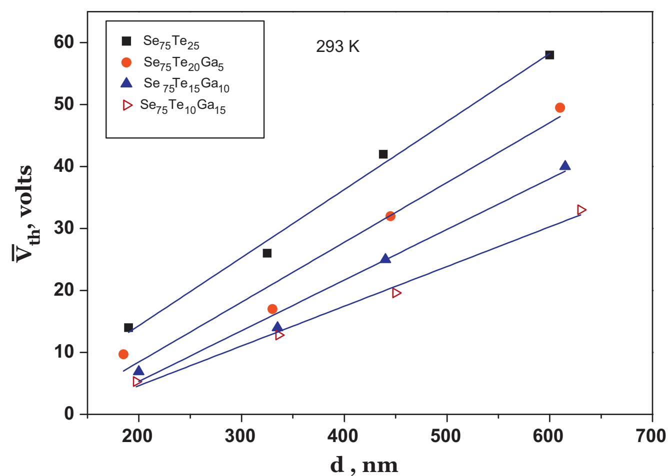

Fig. 6. Thickness dependence of $\bar{V}_{th}$ for $Se_{75}Te_{25-x}Ga_x$ $(0 \leq x \leq 15)$ films at room temperature (293 K).

Table 3
Values of $\bar{F}_{th}$ for $Se_{75}Te_{25-x}Ga_x$ $(0 \leq x \leq 15\%)$ films at room temperature as example.

Composition	$\bar{F}_{th}$ (V/m)
$Se_{75}Te_{25}$	1.10×10^8
$Se_{75}Te_{20}Ga_5$	9.66×10^7
$Se_{75}Te_{15}Ga_{10}$	8.18×10^7
$Se_{75}Te_{10}Ga_{15}$	6.41×10^7

3.3. Thickness dependence of the mean value of threshold switching voltage $\bar{V}_{th}$

The dependence of the threshold voltage V_{th} on the film thickness was examined for the compositions under consideration. The *I*–*V* curves were measured for every film sample at different points uniformly distributed throughout the film surface. *I*–*V* characteristic curves for which V_{th} are equal to the corresponding mean value $\bar{V}_{th}$ for $Se_{75}Te_{20}Ga_5$ films of different thicknesses in the range (185–630 nm) obtained at room temperature are illustrated in Fig. 5 as an example. Fig. 6 shows the variation of the mean value of the threshold switching voltage $\bar{V}_{th}$ with film thickness (*d*), for all investigated film compositions at 293 K as example, indicating a linear relationship in the considered range of thickness. It is observed that $\bar{V}_{th}$ increases with the film thickness due to the increase of film resistance. The slope of the obtained lines represents the mean value of the threshold field $\bar{F}_{th}$ as given in Table 3. The observed relation of the thickness dependence of $\bar{V}_{th}$ agrees with those obtained before for different amorphous system [30,31,39].

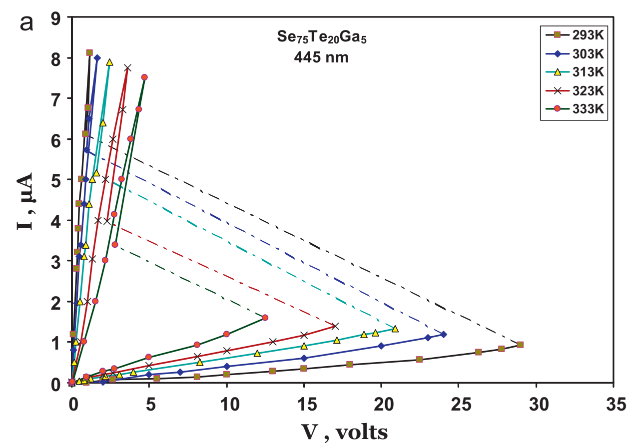

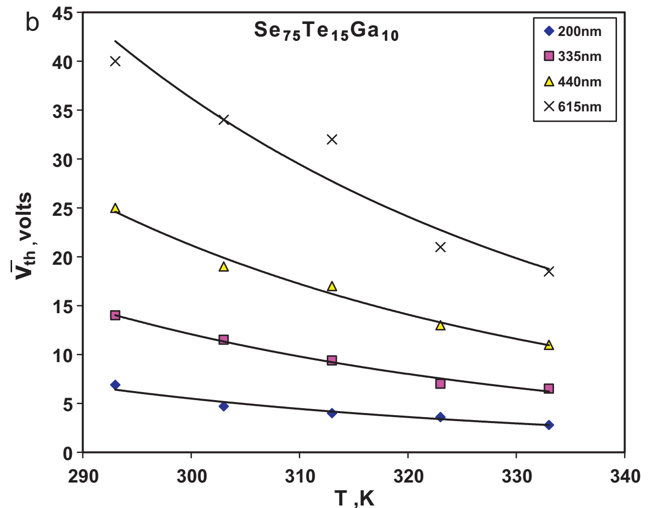

Fig. 7. (a) *I*–*V* characteristic curves for $Se_{75}Te_{20}Ga_5$ films at different temperatures of thickness 445 nm. (b) Plots of $\bar{V}_{th}$ versus temperature for $Se_{75}Te_{15}Ga_{10}$ films of different thicknesses.

3.4. Temperature dependence of the threshold switching voltage $\bar{V}_{th}$

Measurements of the temperature dependence of $\bar{V}_{th}$ for the films studied were carried out through the temperature range (293–333 K) below the corresponding T_g. The obtained curves are illustrated in Fig. 7(a) for $Se_{75}Te_{20}Ga_5$ of thickness (445 nm) as an example. It is clear from these curves that $\bar{V}_{th}$ decrease with increasing temperature in the investigated temperature range. If the ambient temperature increases, the thermal energy required for the transformation of the conduction path material (filament) from the amorphous to the crystalline state will be lower. Therefore, the magnitude of the threshold voltage $\bar{V}_{th}$ decreases with increasing the ambient temperature [32]. The same behavior was obtained for all films of the studied compositions and agrees with the previous observations for other materials [30,31,39–41].

It is known that most of amorphous materials contain dipoles dispersed randomly through out the amorphous matrix. As the electrical field is applied, these dipoles tend to orient themselves in the direction of the field. The orientation process depends on the viscosity of the amorphous matrix as well as on the applied field [39,41]. As the temperature of the conduction path increases

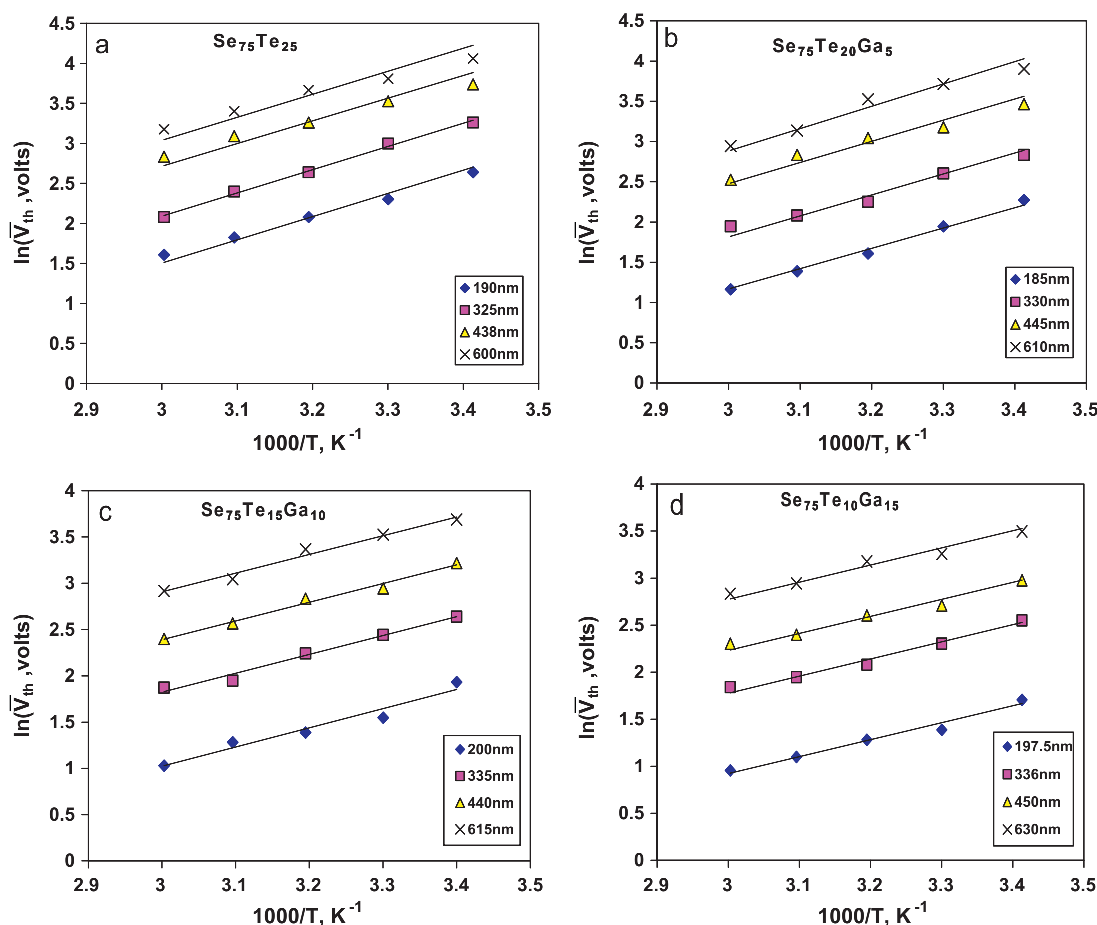

Fig. 8. (a–d) Plots of ln $\bar{V}_{th}$ versus 1000/T for $Se_{75}Te_{25-x}Ga_x$ ($0 \le x \le 15$) films of different thicknesses.

Table 4
Values of ε_{th} and $\varepsilon_{th}/\Delta E_\sigma$ for $Se_{75}Te_{25-x}Ga_x$ ($0 \le x \le 15\%$) films.

Composition	ε_{th} (eV)	$\varepsilon_{th}/\Delta E_\sigma$
$Se_{75}Te_{25}$	0.25 ± 0.006	0.49
$Se_{75}Te_{20}Ga_5$	0.24 ± 0.023	0.49
$Se_{75}Te_{15}Ga_{10}$	20 ± 0.0062.0	0.5
$Se_{75}Te_{10}Ga_{15}$	0.17 ± 0.0024	0.51

its viscosity decreases, which leads to an increase in the orientation process up to the threshold switching point. At this point, the resultant force of the resistance for dipole orientation in viscous amorphous medium diminishes. Thus as the ambient temperature increases the viscosity of the conduction path decreases and the field required to cause maximum dipole orientation would decrease and switching takes place.

Values of $\bar{V}_{th}$ as a function of temperature are recorded for all films of the studied compositions. Fig. 7(b) gives the temperature dependence of $\bar{V}_{th}$ for $Se_{75}Te_{15}Ga_{10}$ films in the thickness range (200–615 nm) as an example. It is clear from this figure that $\bar{V}_{th}$ decreases exponentially with increasing temperature. Plots of $\ln \bar{V}_{th}$ versus $1000/T$ for the considered thin film samples of different thicknesses for the compositions under test are illustrated in Fig. 8(a–d). The obtained relations yield straight lines satisfying the following relation [31]:

$$V_{th} = V_0 \exp\left(\frac{\varepsilon_{th}}{k_B T}\right), \quad (2)$$

where V_0 is a constant and ε_{th} is the threshold voltage activation energy. The obtained straight lines are parallel indicating that ε_{th} is single valued independent of sample thickness in the temperature and thickness ranges mentioned above. Values of ε_{th} are calculated from the slopes of the straight lines of Fig. 8(a–d) and given in Table 4. Values of the ratio $\varepsilon_{th}/\Delta E_\sigma$ for all investigated compositions are calculated and listed also in Table 4. The mean value of this ratio ($\varepsilon_{th}/\Delta E_\sigma \approx 0.5$) is in agreement with that obtained previously [30,31,40,42] for other amorphous semiconductor films. It is also in good agreement with the value of $\varepsilon_{th}/\Delta E_\sigma$ derived theoretically on the basis of the electrothermal model for the switching process [42].

The threshold field $\bar{F}_{th} = \bar{V}_{th}/d$ was deduced at the threshold voltage point at different temperature values for the studied film samples. Fig. 9(a–d) represents the temperature dependence of $\bar{F}_{th}$ for $Se_{75}Te_{25-x}Ga_x$ ($0 \le x \le 15$) film compositions. This figure declares that the electric field decreases with the increase of temperature. It was suggested that at the switching point, the force extracted from the applied field is equal to the restoring force due to the viscosity of the investigated sample. Therefore, in order to keep the electric field constant at threshold switching point at a certain temperature, the sample undergoes switching to the ON-state.

From the above analysis in this section it is concluded that the threshold voltage for the pre-switching region is strongly temperature dependent, and the switching process can be understood in terms of electrothermal process based on Joule heating effect [30,40]. The temperature of the semiconductor is raised due to Joule heating and the conduction process in an amorphous material is an activated type [43]. So, the conductivity of the sample will increase due to the effect of heating. This will allow more current to flow through the heated region and allow more Joule heating, resulting in a further increase in the current density. This will lead to a large electronic contribution to thermal conductivity which enhances

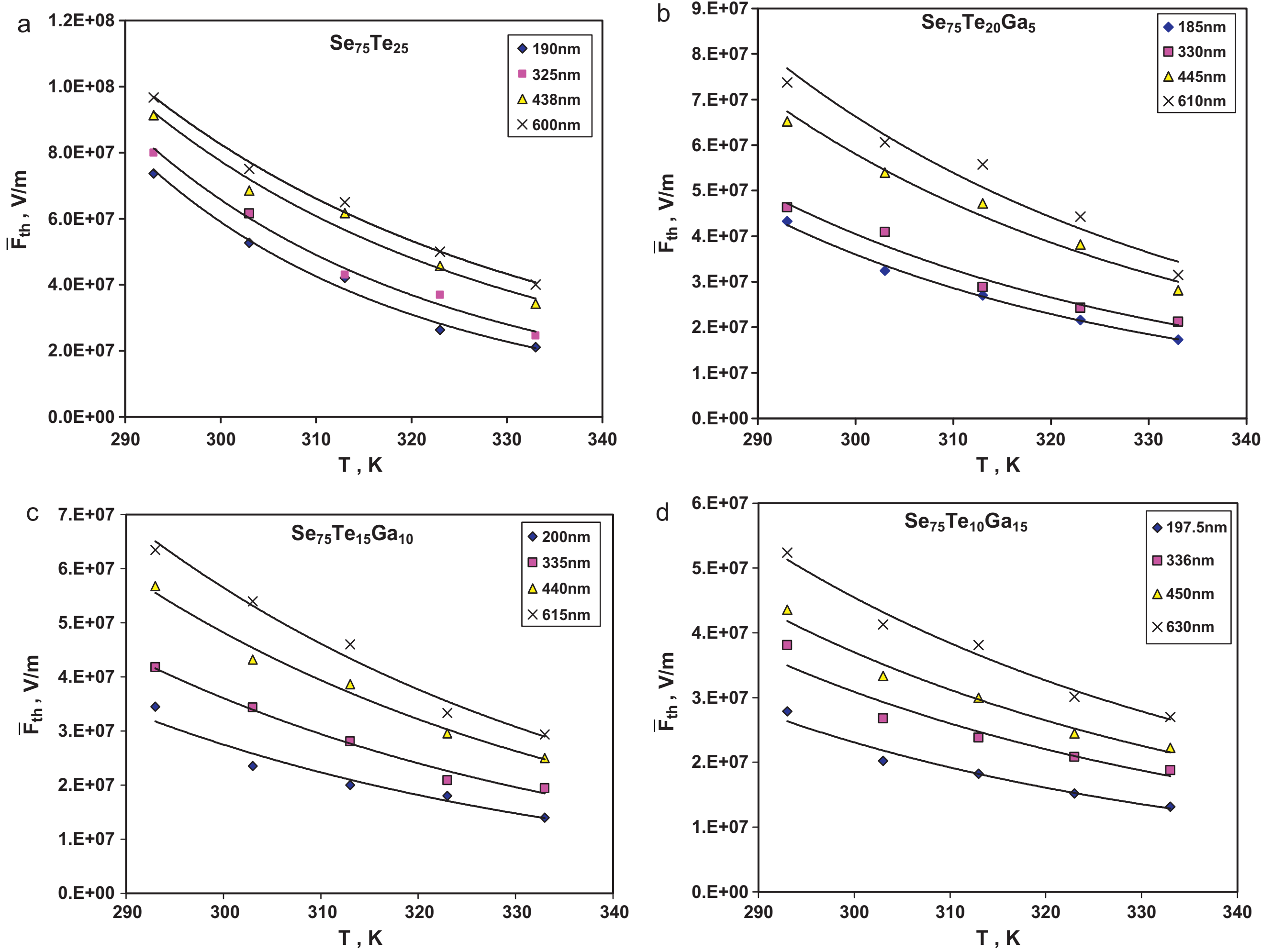

Fig. 9. (a–d) Plots of $\overline{F}_{th}$ versus temperature for $Se_{75}Te_{25-x}Ga_x$ ($0 \le x \le 15$) films of different thicknesses.

the Joule heating in the current filament. Ultimately, the temperature rise will become adequate to initiate the thermal breakdown owing to the strong temperature dependence of the conductivity. A stationary state is reached when the heat lost by conduction from the current filament becomes equal to the Joule heat generated in the heated region.

Finally, it is suggested that the memory-switching phenomenon is caused by a phase change of the material between the electrodes from amorphous to crystalline state due to Joule heating and can be understood in terms of the electrothermal model.

The electrothermal model can be solved to a certain extent by finding a stationary state solution for the heat transport equation [30]

$$C\left(\frac{dT}{dt}\right) = \sigma_{dc}F_{th}^2 + \nabla\cdot(\psi\nabla T), \quad (3)$$

where C is the heat capacity of the sample, ψ is the thermal conductivity coefficient of the samples, F_{th} is the electrical field intensity and σ the electrical conductivity of the sample given by the following equation:

$$\sigma = \sigma_o \exp\left(\frac{-\Delta E_\sigma}{k_B T}\right), \quad (4)$$

The charge conservation equation is given as:

$$\nabla F = -\frac{1}{\sigma_{dc}}\cdot\frac{d\rho}{dt}, \quad (5)$$

where ρ is the charge density, and σ_o is constant. In the case of steady state breakdown, the time derivative of temperature dT/dt can be neglected for the solution of Eq. (3), then the heat conduction equation for a small difference $\Delta T_{breakdown} = T_m - T_s$ between the temperature in the middle of the specimen T_m and that of its surface T_s becomes [38,39]:

$$8\psi\left(\frac{\Delta T}{d^2}\right) + \sigma F_{th}^2 = 0, \quad (6)$$

where d is the thickness of the sample. Steady state breakdown occurs when the amount of heat generated by Joule heating in the specimen cannot be removed by thermal conduction, and the temperature difference for breakdown obtained with the help of Eqs. (4) and (6) is given by:

$$\Delta T_{breakdown} = \frac{T^2 k_B}{\Delta E_\sigma}, \quad (7)$$

where T is the surrounding temperature of the specimen. According to Eq. (7) and using the value of ΔE_σ given in Table 2 values of $\Delta T_{breakdown}$ were calculated for the investigated film compositions at different temperatures in the range (293–333 K).

The obtained values, given in Table 5 are in good agreement with those obtained for other amorphous semiconductor films [30,31,39,42]. Also taking into account the agreement of the obtained values of the ratio $\varepsilon_{th}/\Delta E_\sigma$ given in Table 4 with both the values obtained earlier and value derived theoretically [42] for the breakdown process, it can be concluded

Table 5
Values of $\Delta T_{breakdown}$ at different temperature for $Se_{75}Te_{25-x}Ga_x$ ($0 \le x \le 15\%$) films.

T (K)	$\Delta T_{breakdown}$ (K)			
	$Se_{75}Te_{25}$	$Se_{75}Te_{20}Ga_5$	$Se_{75}Te_{15}Ga_{10}$	$Se_{75}Te_{10}Ga_{15}$
293	14.52	15.1	18.51	22.44
303	15.53	16.2	19.8	24
313	16.57	17.25	21.13	25.61
323	17.64	18.37	22.5	27.27
333	18.75	19.52	23.91	28.98

that the observed memory type switching in the studied films can be satisfactorily explained according to the electrothermal breakdown process. It is clear from the above studies that the addition of Ga to Se–Te system leads to pronounced decrease in all the obtained parameters. This can be explained as follows.

The glass transition temperature shows a decreasing trend with increasing the concentration of Ga impurity in Se–Te samples. This could be explained on the basis of structure changes due to the introduction of Ga atoms. It is known that glassy Se have a ring structure (40% of atoms) and chain structure of about (60% of the atoms). The structure of Se–Te system prepared by quenching is regarded as a mixture of Se_8 rings, Se_6Te_2 rings and copolymer chains. Tellurium enters as copolymer chains and tends to reduce the number of Se_8 rings [44]. In the present case, the addition of Ga occurs at the cost of Te concentration, it also makes bond with Se and Te is dissolved in Se chains. Thus, the numbers of Se_8 rings increases while the number Se–Te copolymer chains and Se–Te mixed rings decreases. Ga atoms bond strongly to Se–Te chains in the system under test. This will lead to increasing the number of Se_8 rings and decreasing the number of long Se–Te polymeric chains and Se–Te mixed rings decreases. Since T_g increases with increasing chain length and decreases with increasing ring concentration [45,46]. Therefore it is expected that T_g to decrease with increasing of Ga concentration in the studied film compositions. Since T_g reflects the rigidity of the lattice [47] thus, it is expected that the rigidity of the lattice of the studied system decreases with increasing Ga content in the studied system.

The presence of Ga addition might increase the concentration of charge carriers increasing the conductivity and there may be a shift in Fermi level [48–50]. It is also assumed that the addition of Ga to Se–Te system leads to a cross linking of the Se–Te chains reducing the disorder of the system which lead a decrease in short-range bonding and making the films less amorphous. This is confirms the observed decrease in ΔE_σ and V_{th} for the considered film compositions.

4. Conclusion

In the above sections the measurements of I–V characteristics of thermally evaporated $Se_{75}Te_{25-x}Ga_x$ ($0 \le x \le 15$ at.%) thin films showed a typical memory type switches. The mean value of the threshold voltage $\bar{V}_{th}$ increases linearly with film thickness through the measured range of thickness, while it decreases exponentially with increasing temperature in the investigated temperature range. The conduction activation energy ΔE_σ, the threshold voltage activation energy ε_{th} and the threshold field $\bar{F}_{th}$ decreases with increasing Ga content in the studied films. The data obtained for switching characterization were explained according to the electrothermal model initiated from Joule heating of current channel.

References

[1] A.J. Savage, Infrared Optical Materials and their Antireflection Coating, Hilger, London, 1985.
[2] S.V. Shiryaev, C. Boussard-Pl'edel, P. Houizot, T. Jouan, J.L. Adam, J. Lucas, Mater. Sci. Eng. B 127 (2006) 138.
[3] F. Wang, Z. Zhang, R. Liu, X. Wang, X. Zhu, A. Pan, et al., Nanotechnology 18 (2007) 305705.
[4] B.T. Kolomiets, Phys. Status Solidi 7 (1964) 713.
[5] P. Nagel, H. Ticha, L. Tichy, A. Triska, J. Non-Cryst. Solids 59 (1983) 1015.
[6] N. Tohge, H. Matsuuo, T. Minami, J. Non-Cryst. Solids 95 (1987) 809.
[7] S. Kohli, V.K. Sachdeva, R.M. Mehra, P.C. Mathur, Phys. Status Solidi B 209 (1998) 389.
[8] M.A. Majeed, M. Zulfequar, A. Kumar, M. Husain, J. Mater. Chem. Phys. 87 (2004) 179.
[9] E. Maruyama, Jpn. J. Appl. Phys. 21 (1982) 213.
[10] K. Tanaka, A. Odayime, J. Appl. Phys. Lett. 38 (1981) 481.
[11] K. Tada, W. Tanino, T. Murai, M. Aoki, Thin Solid Films 96 (1982) 141.
[12] S.R. Ovshinsky, Phys. Rev. Lett. 21 (1968) 1450.
[13] M. Horie, T. Ohno, N. Nobukuni, K. Kioyo, T. Hahizume, Tech. Digest, ODS2001 MC1 (2001) 37.
[14] T. Akiyama, M. Uno, H. Kituara, K. Narumi, K. Nishiuchi, N. Yamada, Jpn. J. Appl. Phys. 40 (2001) 1598.
[15] T. Ohta, J. Opto-Electron. Adv. Mater. 3 (2001) 609.
[16] S. Lai, Tech. Dig. Int. Electron Devices Meet. (2003) 255.
[17] G. Servalli, IEDM Tech. Dig. (2003) 113.
[18] M.A. Majeed Khan, M. Zulfequar, M. Husain, Mater. Lett. 57 (2003) 2894.
[19] S.A. Fayek, Vacuum 72 (2004) 11.
[20] A.A. Joraid, Thermochim. Acta 456 (2007) 1.
[21] G.A.M. Amin, A.F. Maged, Mater. Chem. Phys. 97 (2006) 420.
[22] Z.H. Khan, M. Zulfequar, M. Manzer Malki, M. Husain, Mater. Sci. Technol. 13 (1997) 484.
[23] Z.H. Khan, M. Zulfequar, M. Ilyas, M. Husain, Acta Phys. Pol. A 98 (2000) 93.
[24] M. Okuda, F.S. Jiang, J.C. Rhee, T. Matsushita, J. Non-Cryst. Solids 97–98 (1987) 1351.
[25] (a) T. Matsushita, A. Suzuki, M. Okuda, H. Naito, T. Nakau, Jpn. J. Appl. Phys. 22 (1983) 760;
(b) T. Matsushita, A. Suzuki, M. Okuda, H. Naito, T. Nakau, Jpn. J. Appl. Phys. 24 (1985) L504.
[26] J.C. Rhee, M. Okuda, T. Matsushita, Jpn. J. Appl. Phys. 26 (1987) 102.
[27] S. Kumar, M. Husain, M. Zulfequar, Physica B 387 (2007) 400.
[28] A.S. Maan, D.R. Goyal, India J. Phys. 63 (1989) 457.
[29] A.S. Maan, D.R. Goyal, A. Kumar, Rev. Phys. Appl. 24 (1989) 613.
[30] R.M. Mehra, R. Shyan, P.C. Mathur, J. Non-Cryst. Solids 31 (1979) 435.
[31] M.A. Afifi, N.A. Hegab, H.E. Atyia, A.S. Farid, J. Alloys Compd. 463 (2008) 10.
[32] M.P. Slankamenac, S.R. Lukíc, M.B. Živanov, Semicond. Sci. Technol. 24 (2009) 085021.
[33] D. Adler, M.S. Shur, M. Silver, S.R. Ovshinsky, J. Appl. Phys. 51 (1980) 3289.
[34] D. Adler, Sci. Am. 36 (1977) 236.
[35] H. Fritzsche, S.R. Ovshinsky, J. Non-Cryst. Solids 4 (1970) 464.
[36] A. Tolansky, Introduction to Interferometry, Longman, New York, 1951.
[37] D. Alder, S.C. Moss, J. Vac. Sci. Technol. 9 (1972) 1182.
[38] N.F. Mott, Philos. Mag. 19 (1969) 835.
[39] A.E. Bekheet, Eur. Phys. J. Appl. Phys. 16 (2001) 187.
[40] K. Shimakawa, Y. Iragaki, T. Arizumi, Jpn. J. Appl. Phys. 12 (1973) 1043.
[41] M.M. Abdel-Aziz, Appl. Surf. Sci. 253 (2006) 2059.
[42] M.A. Afifi, N.A. Hegab, Vacuum 48 (1997) 135.
[43] H.J. De Wit, C. Creveccoeur, Solid State Electron. 15 (1972) 729.
[44] A.T. Ward, J. Phys. Chem. 74 (1970) 4110.
[45] A. Eisenbery, Polym. Lett. 1 (1963) 177.
[46] Houfu Li, Zhimin Wang, Xiyun Yuan, J. Zhengzhou, Inst. Light Ind. 9 (1994) 89 (In Chinese).
[47] A. Giridhar, P.C.L. Narasimham, S. Mahadevan, J. Non-Cryst. Solids 43 (1981) 29.
[48] M.M. Malik, M. Zulfequar, A. Kumar, M. Husain, J. Phys. Condens. Matter 4 (1992) 8331.
[49] S. Okano, et al., J. Non-Cryst. Solids 59 and 60 (1983) 969.
[50] R. Arora, A. Kumar, J. Mater. Sci. Lett. 9 (1990) 348.